

# Simulating the Effects of Switching Events on Transformers

H. W. Dommel and M. B. Selak  
Power Systems Consultants  
4427 West 6<sup>th</sup> Avenue  
Vancouver, B.C., Canada V6R 1V2

D. Nikolic and P. Vujovic  
Electric Power Research Institute  
3412 Hillview Avenue  
Palo Alto CA 94304-1395, U.S.A.

**Abstract** - This paper describes transformer models for various types of switching events, which can have an impact on transformers, with respect to relay protection and overvoltage surge arrester protection. For relay protection, the prediction of inrush currents is important. For surge arrester protection, the magnitude and steepness of transient overvoltages are the important factors. Overvoltages can be created by transients from capacitor switching in nearby substations. Overvoltages can also appear during interruption of the small inductive excitation currents. Remote energization of transformers through short overhead lines or short underground cables can create travelling wave phenomena with frequencies which can be close to resonance frequencies of the transformer. This situation can lead to internal winding resonances. The simulation of these phenomena in the time domain, and the assessment of resonance phenomena in the frequency domain, are briefly described.

**Keywords:** Transient Analysis, Transformer Models, Switching, EMTP.

## I. INTRODUCTION

Transformers must be able to withstand the stresses imposed on them by switching events in the electric power network. For the simulation of such events, transformer models are needed which are appropriate for the particular type of study. In the simplest case, the switching transients contain low frequencies close to the power frequency, as in fault current and inrush current studies. In more complicated cases, high frequencies above a few kHz to a few hundred kHz may appear.

Starting from the basic linear low frequency model of the transformer, the inclusion of saturation effects, and modifications needed for high frequency behaviour are briefly discussed. Some examples of less common switching events are used to illustrate the practical importance of switching events, to avoid damage to transformers.

## II. BASIC TRANSFORMER MODEL

### A. Representation of short-circuit impedances

The basic transformer model can be derived from the short-circuit impedance data in the form of a system of branch equations for the N windings of the transformer,

$$[v] = [R][i] + [L]\left[\frac{di}{dt}\right]$$

where  $[v]$  and  $[i]$  are the vectors of the voltages across and the currents through the N windings, and  $[R]$  and  $[L]$  are the resistance and inductance matrices for the N windings.

If the exciting current is ignored, which is done in many types of studies, the inductance matrix  $[L]$  becomes infinite. It is therefore preferable to work with the alternative equation

$$[L]^{-1}[v] = [L]^{-1}[R][i] + \left[\frac{di}{dt}\right], \quad (1)$$

in which the inverse inductance matrix  $[L]^{-1}$  now always exists. It becomes singular when the exciting current is ignored, but this does not cause any problems in solutions based on nodal equations. Both  $[R]$  and  $[L]^{-1}$  can be found with support programs, such as BCTRAN in EMTP96 and in ATP, or TRAFO and MTDATA in MicroTran [1, p. 6-52]. For steady-state solutions, (1) can easily be re-written as a phasor equation, as explained in [1, p.3-21].

Generally speaking, (1) can be used for single-phase as well as three-phase units. For a three-phase two-winding transformer, the size of the matrices simply becomes  $N=6$ . Theoretically, 15 short-circuit tests could be performed on the six windings. Since such extensive tests are rarely done, the support routines mentioned above use positive and zero sequence short-circuit test data instead, to create the  $[R]$ - and  $[L]^{-1}$ -matrices.

### B. Representation of zero sequence exciting current

For three-legged core three-phase transformers, there is reason to believe that the differences between zero and positive sequence short-circuit test data are mostly caused by the low zero sequence magnetizing inductance, which represents the magnetic path for the three equal fluxes in the three legs, with return through air and the transformer tank. This zero sequence magnetizing inductance  $L_{m-zero}$  is low (typically 30 to 300 %), and more or less linear. It should be connected as a shunt element across the winding farthest from the core, which is usually the high voltage side, with self and mutual reciprocal inductances calculated from  $1/L_{m-zero}$  and  $1/L_{m-pos} = 0$  (Fig. 1).

The support routine TOPMAG [2] has been created to include  $L_{m-zero}$ , and to modify the zero sequence short-circuit inductances for the non-shunt branches accordingly. If  $L_{m-zero}$  is used, the errors in the rest of the model for the non-shunt branches are small if zero sequence values are assumed to be equal to positive sequence values, which means that the

three-phase unit can then be modelled as three single-phase units, together with  $L_{m-zero}$  which couples the three phases. The modifications created by TOPMAG are very important on transformers without delta-connected windings, but less important if delta-connected windings provide another short-circuit path for zero sequence.

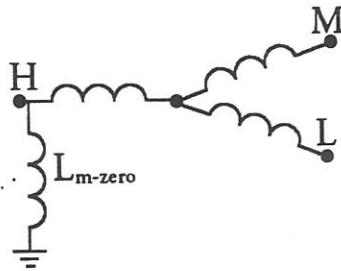


Fig. 1. Zero sequence circuit of three-winding three-legged core transformer (H = high, M = medium, L = low voltage winding); L grounded if L is delta connected.

### C. Connections

No assumptions are made in (1) about the type of connection (wye, delta, or zigzag). The connections are simply introduced through node name assignments to the winding terminals. For an ungrounded wye-connection, the three windings would go "A to N", "B to N", and "C to N". For solid grounding, "N" would be replaced by the name for the ground. There is also no need to worry about the effect which the connection has on the zero-sequence behaviour. If the windings go "A to B", "B to C", and "C to A" in delta connection, the model automatically provides a short-circuit in zero sequence. Also, the phase shift created in wye/delta connections, of  $+\alpha$  in positive sequence and  $-\alpha$  in negative sequence, which converts a single-line-to-ground fault on the wye side into a line-to-line fault on the delta side, is automatically included in the model of (1). The fact that these connection-related characteristics are automatically accounted for is one of the advantages of working in phase quantities rather than in sequence quantities.

The basic model of (1) is usually sufficiently accurate for studies involving fault currents in transformers. An interesting modification of the basic model for internal faults is worth mentioning here [3].

## III. SATURATION EFFECTS AND RESIDUAL FLUX

### A. Magnetizing impedance

For inrush current and ferroresonance studies, the saturation effects of the iron cores have to be included. Tests have shown [4] that it is best to add the nonlinear magnetizing inductance to the model of (1) across the winding closest to the core, which is usually the low voltage winding (Fig. 2). The difference in the saturated slopes between "M" and "L" is very close to the short-circuit inductance  $L_M + L_L$ , and the difference in the saturated slopes between "H" and "L" is very close to the short-circuit inductance  $L_H + L_L$ .

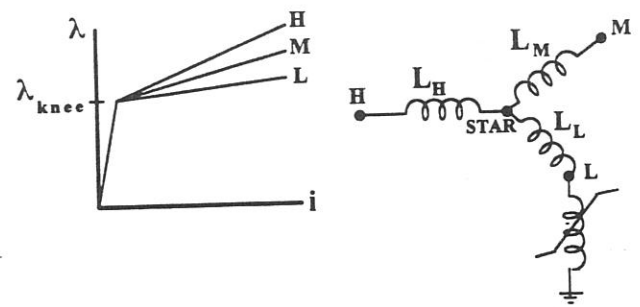


Fig. 2. Placement of magnetizing inductance.

The simplest representation of the saturation effect consists of a two-slope piecewise linear inductance, with an unsaturated value  $L_1$ , which is very high on large transformers, and the saturated "air core" value  $L_2$ , which is of the same order of magnitude as the short-circuit inductance. CIGRE [5] quotes typical values of

$$L_2 = 1.0 \text{ to } 1.5 L_{\text{short-circuit}} \text{ for full windings, and}$$

$$L_2 = 3.0 \text{ to } 4.0 L_{\text{short-circuit}} \text{ for autotransformer windings.}$$

A linear resistance  $R_{Fe}$  in parallel with the magnetizing inductance is sometimes enough to represent the iron core losses approximately. If this is not good enough, more sophisticated models for hysteresis and eddy current losses are available in most versions of the EMTP.

### B. Inrush current

Fig. 3 shows the network configuration of a CIGRE test case for inrush current simulations [6].

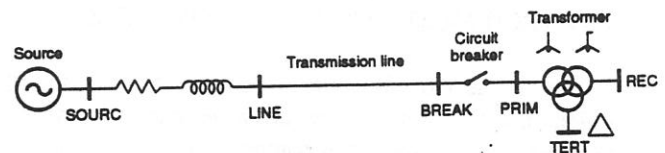


Fig.3. Network configuration for inrush current case.

Fig.4 shows the comparison with field test results for phase C on the primary side [7]. In the simulation with MicroTran, the two-slope inductance mentioned above was used. Iron core losses were ignored. The critical data for coming close to the field test results in this case were the residual fluxes in the three core legs of the transformer, prior to closing the circuit breaker. Their values were repeatedly changed by hand until a good match with field test results was found. Attempts have been made to calculate the residual fluxes with sophisticated hysteresis and eddy current models from a preceding circuit breaker opening simulation, but these attempts have not been completely successful. Since the saturated value  $L_1$  of large transformers is almost infinite, compared to  $L_2$ , it is fairly simple to start with an initial value of residual flux on the flux axis of the nonlinear characteristic [8].

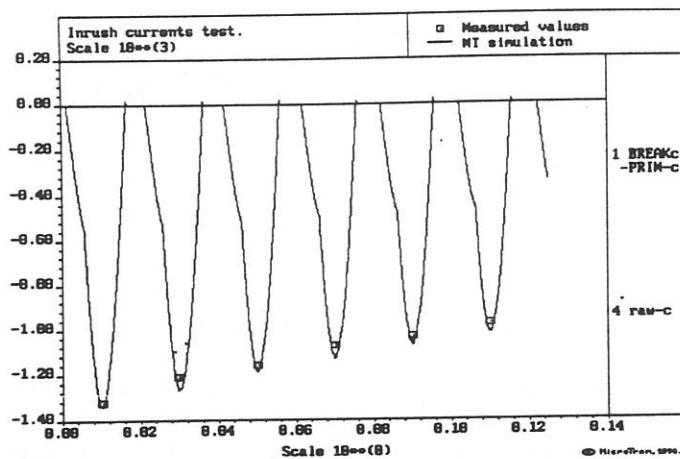


Fig. 4. Inrush current in phase C on the primary side (square boxes in curve show the measured peak values).

### C. Ferroresonance

Ferroresonance studies are usually not as simple as inrush current studies. There are cases where the simple models discussed in Section III.A produce good answers, such as in the case of ferroresonance on the 2.1 km long 1100 kV test line described in [9]. But there are also other cases where small changes in parameters can produce large changes in the results. A good summary of the "art" of ferroresonance studies can be found in [10].

## IV. HIGH-FREQUENCY TRANSFORMER MODELS

For frequencies above a few kHz, it becomes important to take the effect of stray capacitances into account, and if possible, also the increased damping caused by skin effects in the conductors and the eddy current effects in the iron cores. There are essentially two ways to arrive at such high-frequency transformer models: using design data to calculate the stray capacitances (and possibly making some reasonable assumptions about skin effect and eddy currents), or fitting a model to measured frequency response data.

### A. Stray capacitances from design data

It is possible to calculate the stray capacitances from design data of the transformer (geometry, etc.). As suggested in [11] and by others, capacitances should be included,

- $C_a$  between the winding closest to the core and the core, and  $C_d$  between the outer winding and the tank,
- $C_b$  between any two windings,
- $C_c$  across each winding from one end to the other, as shown in Fig. 5.

In reality, inductances and capacitances are distributed, but reasonably accurate results, as seen from the terminals, can be obtained by lumping one half of  $C_a$  and  $C_b$  at each end of the winding, and by lumping the total capacitance  $C_c$  in parallel with the winding. In [11], good agreement between model impedances and measured impedances to frequencies of approx. 100 kHz could be obtained with this approach.

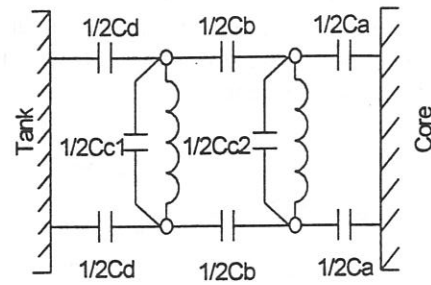


Fig. 5. Addition of capacitances.

To represent the skin effect in conductors requires modifications in the  $[R]$ - and  $[L]^{-1}$ -matrices, e.g., by adding a number of coupled short-circuited coils in parallel with the windings [12], or at least one conductance matrix  $[G]$  in parallel with  $[L]^{-1}$  [1, p. 3-11]. Hysteresis/saturation and eddy currents in the iron core could be modelled the same way as discussed in the next section.

### B. Fitting model to measured data

Ontario Hydro developed a very comprehensive high frequency transformer model, which is based on the frequency characteristics of the transformer admittance matrix  $[Y(\omega)]$  between its terminals [13]. It requires measured data for these frequency-dependent admittances, which may not always be available, except in circumstances where a thorough investigation of a transformer failure justifies the measurement effort [14]. In general, the model shows the behaviour at the terminals only, but in the case of [14], information was also obtained for the internal voltage distribution by making measurements at various points inside the windings. The high frequency model starts from the basic model of (1) by adding extra linear R-L-C networks to it, and by fitting their values in such a way that the frequency behaviour of the model matches the measured admittances closely. These R-L-C networks represent essentially the skin effects in the conductors and the stray capacitance effects.

For more accurate representations of the high frequency eddy current effects in the iron cores, another linear R-L network can be added in parallel to the nonlinear inductance, to replace the simple resistance  $R_{Fe}$  mentioned earlier [15]. The nonlinear inductance can either be the simple two-slope inductance mentioned earlier, or a more sophisticated hysteresis/saturation model, such as the "Type 92 Hysteretic Reactor" in the EMTP version EMTP96.

All three "modules", namely the high frequency transformer module, the eddy current module and the hysteresis/saturation module, are "add-ons" to the basic model of (1) in Ontario Hydro's approach.

For system studies, such "terminal models" are sufficient to show the interaction between the transformer and the power system network. For transformer designers it is also important to have "internal" transformer models, which give information about the internal voltage distribution across windings when the transformer is subjected to high-



frequency transients. To develop such models requires specialized expertise, which only transformer designers have.

## V. EXAMPLES OF SWITCHING PROBLEMS ON TRANSFORMERS

In addition to the low frequency inrush current example shown in Fig. 4, a few other examples are discussed here which involve higher frequencies.

### A. Remote capacitor bank switching

When capacitor banks in a substation are energized directly, without closing resistors or other means for reducing the transients, the voltage at the bus collapses almost instantaneously, and then recovers with oscillations around the power frequency waveshape. An interesting case is discussed in [16]. In that case, a capacitor bank in a 230 kV substation was energized with circuit switchers, which tended to close almost simultaneously in two phases, close to their respective crest voltages. This created a fairly high phase-to-phase voltage spike, which travelled along a radial 230 kV transmission line to a phase shifting transformer in a substation 55.5 km away, and damaged this transformer.

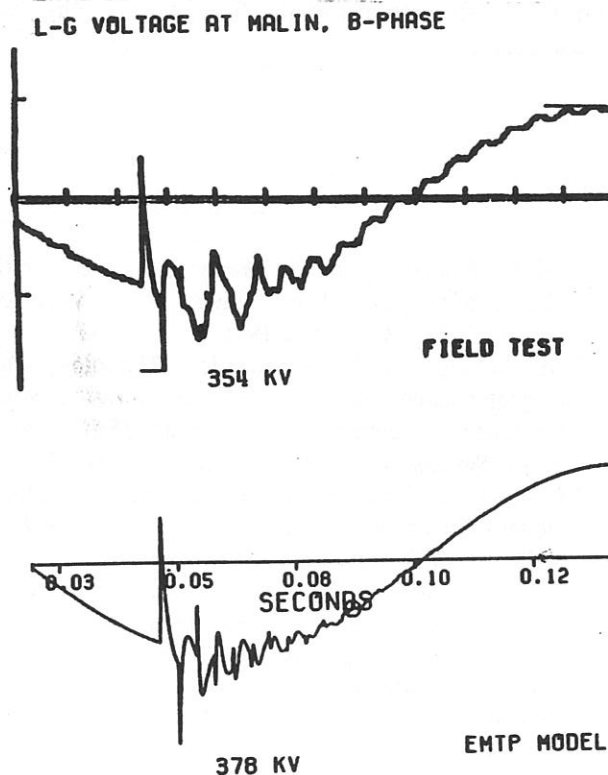


Fig. 6. Field measurement and EMTP simulation of capacitor switching transients.

Fig. 6 shows a comparison between one of the field tests and an EMTP simulation [17]. While the agreement is not perfect, the EMTP results do show the basic phenomena involved in such capacitor switching cases.

These capacitor switching transients can be reduced significantly if closing resistors, controlled closing and/or

series reactors are used. For the latter case, it is important to check whether the L-C combination can create undesirable resonances for inrush currents during energization or for outrush currents when the capacitor bank is switched off.

### B. Remote energization of transformer

If an unloaded transformer is switched remotely through a short overhead line or cable, e.g., from a circuit breaker at "LINE" in Fig. 1, rather than in "BREAK-PRIM", then a travelling wave propagates along the line towards the transformer, which will see the transformer termination as a very high impedance. This creates an oscillation with a frequency of

$$f = \frac{1}{4\tau} \quad (2)$$

which can be close to resonance frequencies of the transformer. A case where an unloaded transformer was switched remotely through a 3.273 km long feeder cable is discussed in [18]. With the velocity of waves in cables being approximately half the speed of light, the travel time for 3.273 km becomes 0.0218 ms, which leads to  $f = 11.46$  kHz. This seems to have been close to a resonant frequency of the transformer, and may have led to the reported damage. [18] explains the basic phenomena with relatively simple formulas, which include the short-circuit inductance and stray capacitances of the transformer. It is a good example that EMTP simulations are not always needed to gain insight.

The same resonance condition can occur with short overhead lines. For a length of 10 km, the corresponding frequency would be 7.5 kHz, which could be in the range of a transformer resonance frequency.

If the overhead line is much longer, then the frequency of (2) becomes very low. For example, a line length of 250 km would have an oscillation frequency of 300 Hz. This is obviously outside the range of transformer resonance frequencies. What could happen in this case, however, is a resonance between the line and the 5<sup>th</sup> harmonic in the transformer exciting current caused by the saturation effect (for a power frequency of 60 Hz). This could lead to what is called "temporary overvoltages" with noticeable distortion of the 60 Hz waveshape.

### C. Interruption of small inductive currents

When an unloaded transformer is switched off, the circuit breaker or circuit switcher must interrupt the exciting current, which is very small on modern transformers with grain-oriented steel. Since the quenching process in the arc of a circuit breaker is designed for high currents, the quenching may become so strong for small inductive currents that the current is "chopped". It then drops almost instantaneously from a certain value of current to zero, rather than being interrupted at the next natural current zero crossing. In reality, the chopping is not instantaneous, of course, but a damped oscillation with a high frequency. This chopping can in turn produce overvoltages.

In most EMTP versions it is possible to specify a chopping value. The current will then drop from that value to zero within one time step  $\Delta t$ . This may be reasonable enough, but more sophisticated approaches can be used as well, with a slower drop to the zero value.

In switching off an unloaded transformer, the overvoltages are created by the transfer of energy  $\frac{1}{2}L_m i^2$  in the magnetizing inductance into energy  $\frac{1}{2}Cv^2$  in the transformer stray capacitance, or in the case of connected capacitor banks, primarily into the capacitances of the transformer banks. The simplest model is a magnetizing inductance  $L_m$  in parallel with a stray capacitance  $C$ . In that case the overvoltage becomes

$$v = i_{chop} \cdot \sqrt{\frac{L_m}{C}} \quad (3)$$

where  $i_{chop}$  is the value where the current is being chopped.

Notice that the overvoltage in (3) is independent of the operating voltage, and depends only on the current  $i_{chop}$ , and on what one could call the surge impedance  $\sqrt{L_m/C}$  of the transformer [19]. This is of course an oversimplification, because the exciting current depends on the voltage rating, though the value where the exciting current gets chopped may not depend that much on the ratings. The chopping current value depends more likely on the characteristics of the circuit breaker or circuit switcher.

In terms of per unit overvoltage, higher values are to be expected for the lower voltage ratings, based on (3). This has been verified in the tests reported in [20]. For an operating voltage of 100 kV, a 3.3 p.u. overvoltage is shown in the trend curve, while at 400 kV it is approx. 1.8 p.u.

Happoldt and Oeding mention in their book published in 1978 [21] that "the much discussed problem of earlier years of switching off unloaded transformers has more or less lost its importance today, because the cold-rolled (probably means 'grain-oriented') steel used nowadays produces much lower exciting current". With higher  $L_m$ , the resonance frequency decreases as well, and with it the overvoltage.

[21] does mention that higher overvoltages can still be expected today if a transformer is switched off that has shunt reactors connected to it. An example for such a case is shown in [20]. A very active CIGRE Working Group looked into the interruption of small inductive currents in the 1980's, with major emphasis on shunt reactor switching [22].

## VI. FREQUENCY SCANS

Most EMTP versions have an option for steady-state solutions. This option was originally included to start transient simulations from proper steady-state initial conditions. By varying the frequency and calling the steady-state solution routine repeatedly, it becomes easy to obtain the frequency response of the network. Such "frequency scans" are useful for finding potential resonances in the

network. Frequency scans are normally used to compare the frequency response of high-frequency transformer models, discussed in Section IV-B, against measured data. Another application of frequency scans in the lower frequency region would be the analysis of potential resonances between a transformer and nearby shunt capacitors or series capacitors. In this case, a low-frequency transformer model without stray capacitances would probably be accurate enough. Frequency scans in the low frequency region are also useful in power systems with power electronics devices, where low frequency resonances must be taken into account in the proper design of the control system.

## VII. CONCLUSIONS

While the basic low frequency model of the transformer is adequate for many power system transient studies, there are switching events where more accurate transformer models are needed. For the energization of unloaded transformers, the inclusion of saturation effects is obviously important. For switching events which generate high frequency transients, high frequency transformer models are needed which include the effects of stray capacitances, of skin effects in the conductors, and eddy current effects in the iron core. Some examples of high frequency switching events are discussed.

## VIII. REFERENCES

- [1] H.W. Dommel, *EMTP Theory Book*, 2<sup>nd</sup> edition. Microtran Power System Analysis Corp., Vancouver, Canada, 1992; latest update 1996.
- [2] A. Narang and R. H. Brierley, "Topology based magnetic model for steady-state and transient studies for three-phase core type transformers", *IEEE Trans. on Power Systems*, vol. 9, Aug. 1994, pp. 1337-1349.
- [3] P. Bastard, P. Bertrand, and M. Meunier, "A transformer model for winding fault studies", *IEEE Trans. on Power Delivery*, vol. 9, April 1994, pp. 690-699.
- [4] E. P. Dick and W. Watson, "Transformer models for transient studies based on field measurements", *IEEE Trans. on Power Apparatus and Systems*, vol. PAS-100, Jan. 1981, pp. 409-419.
- [5] CIGRE Working Group 33.02, *Guidelines for Representation of Network Elements when Calculating Transients*. Technical Brochure CE/SC GT/WG 02, Paris, 1990.
- [6] B. Holmgren, R. S. Jenkins, and J. Riubrugent, "Transformer inrush current", CIGRE Report 12-03, Paris, 1968.
- [7] *Transformer Inrush Current, Test Case 1*. Microtran Power System Analysis Corp. Vancouver, Canada, Dec. 1990.
- [8] *MicroTran Reference Manual*. Microtran Power System Analysis Corp. Vancouver, Canada, Sept. 1992.

- [9] H. W. Dommel, *Case Studies for Electromagnetic Transients*. Microtran Power System Analysis Corp., Vancouver, Canada, 1993 (this publication has also been used over many years in EMTP Short Courses at the University of Wisconsin, Madison, Wisconsin, U.S.A.).
- [10] IEEE Task Force, "Modeling and analysis guidelines for slow transients - part III: the study of ferroresonance", *IEEE Trans. on Power Delivery*, vol. 15, Jan. 2000, pp. 255-265.
- [11] T. Adielson, A. Carlson, H. B. Margolis, and J. A. Halladay, "Resonant overvoltages in EHV transformers - modeling and application", *IEEE Trans. on Power Apparatus and Systems*, vol. PAS-100, July 1981, pp. 3563-3572.
- [12] E. E. Mombello, "New power transformer model for the calculation of electromagnetic resonant transient phenomena including frequency-dependent losses", *IEEE Trans. on Power Delivery*, vol. 15, Jan. 2000, pp. 167-174.
- [13] A. S. Morched, L. Marti, and J. H. Ottevangers, "A high frequency transformer model for the EMTP", *IEEE Trans. on Power Delivery*, vol. 8, July 1993, pp. 1615-1626.
- [14] A. S. Morched, L. Marti, R. H. Brierley, and J. G. Lackey, "Analysis of internal winding stresses in EHV generator step-up transformer failures", vol. 11, April 1996, pp. 888-894.
- [15] E. J. Tarasiewicz, A. S. Morched, A. Narang, and E. P. Dick, "Frequency dependent eddy current models for nonlinear iron cores", *IEEE Trans. on Power Systems*, vol. 8, May 1993, pp. 588-597.
- [16] R. S. Bayless, J. D. Selman, D. E. Truax, and W. E. Reid, "Capacitor switching and transformer transients", *IEEE Trans. on Power Delivery*, vol. 3, Jan. 1988, pp. 349-357.
- [17] R. Hasibar, "Typical studies made with the EMTP on the BPA power system", *Class notes for EMTP Short Course*, University of Wisconsin, Madison, WI, U.S.A., 1987.
- [18] G. Ch. Paap, A. A. Alkema, and L. van der Sluis, "Overvoltages in power transformers caused by no-load switching", *IEEE Trans. on Power Delivery*, vol. 10, Jan. 1995, pp. 301-306.
- [19] A. Greenwood, *Electrical Transients in Power Systems*, Wiley, New York, 1991.
- [20] M. Erche, "Switching surges". Chapter in R. Ragaller, *Surges in High-Voltage Networks*, Plenum Press, New York, 1980.
- [21] H. Happoldt and D. Oeding, *Elektrische Kraftwerke und Netze*, Springer, Berlin, 1978.
- [22] CIGRE Working Group, "Interruption of small inductive currents; Chapters 1 and 2", *Electra*, Oct. 1980, pp. 73-103.